CDF/JET/PHYS/PUBLIC/8381
Version 1.0
July 15, 2006

Measurement of the inclusive $\mathbf{W^{\pm} \to e^{\pm}\nu}$ + n jet cross section in $\mathbf{p\bar{p}}$ collisions at $\mathbf{\sqrt{s} = 1.96}$ TeV

Ben Cooper[a], **Andrea Messina**[b1], **David Waters**[a]
on behalf of the CDF collaboration
[a] *University College London, UK*
[b] *INFN, Rome, Italy*

Abstract

The measurement of the cross section for the inclusive production of W bosons in association with jets in $p\bar{p}$ collisions at $\sqrt{s} = 1.96$ TeV using the Collider Detector at Fermilab (CDF II) is presented. It is based on an integrated luminosity of 320 pb^{-1}, and includes events with up to 4 or more jets. In each jet multiplicity sample the differential and cumulative cross sections with respect to the transverse energy of the $i^{th}-$jet are measured. For $W + 2$ jet the differential cross section with respect to the 2-leading jets invariant mass $m_{j_1 j_2}$ and angular separation $\Delta R_{j_1 j_2}$ is also reported. The data are compared to predictions from Monte Carlo simulations.

The study of jets produced in events containing a W bosons provides a useful test of Quantum Chromo-Dynamics (QCD) at high momentum transfers. Recently a lot of work has been channeled to develop sophisticated Monte Carlo programs capable of handling more particle in the final state at the leading order (LO), or in some cases, next-to-leading order (NLO) [1]. Measurements of $W+$ jet cross sections are an important test of QCD and may be used to validate these new approaches. A good understanding of $W+$ jet production is vital to reduce the uncertainty on the background to top pair production and to increase the sensitivity to higgs and new physics searches at the Tevatron and the LHC.

This note describes a new measurement of the $W+$ jet cross section as a function of relevant jet kinematic variables. Similar measurements have been carried out in the past for $W + n$ jet (with $n \geq 1,\ 4$) production inclusively [2] and, for $W + 1$ jet, as a function of the minimum jet transverse energy $E_T^{jet}$from 15 to 95 GeV [3]. The measurement presented here extends that region up to 195 GeV, and provides differential and cumulative cross sections as a function of the E_T of the first, second, third, and fourth leading jet. Cross sections have been corrected to particle level jets, and are defined within a limited W decay phase space, closely matching that which is experimentally accessible. This definition, easily reproduced theoretically, minimises the model dependence that can enter a correction back to the full W cross-section. This analysis is based on 320 ± 18 pb^{-1} of data collected by the upgraded Collider Detector at Fermilab during the Tevatron Run II period. The CDF II detector [4] is an azimuthally and forward-backward symmetric apparatus situated around the $p\bar{p}$ interaction region, consisting of a magnetic spectrometer surrounded by calorimeters and muon chambers. $W \to e\nu$ candidate events are selected from a high E_T electron trigger ($E_T^e \geq 18$ GeV, $|\eta^e| < 1.1$) by requiring one good quality electron candidate ($E_T^e \geq 20$ GeV) and the missing transverse energy ($\not\!\!E_T$) to be greater than 30 GeV. The $W \to e\nu$ candidate events are then classified according to their jet multiplicity into four n$-$jet samples ($n \geq 1,\ 4$). Jet are searched for using an iterative seed-based cone algorithm [5], with a cone radius $R = \sqrt{(\Delta\eta)^2 + (\Delta\phi)^2} = 0.4$. Jets are

[1]Corresponding authors, e-mail : messina@fnal.gov, bdc@hep.ucl.ac.uk

requested to have a corrected transverse energy $E_T^{jet} > 15$GeV and a pseudorapidity $|\eta| < 2.0$. E_T^{jet} is corrected on average for the calorimeter response and the average contribution to the jet energy from additional $p\bar{p}$ interaction in the same bunch crossing [6]. Backgrounds can be classified in two categories: QCD and W-like events. The latter is represented by events which manifest themselves as real electrons and/or $\not\!\!E_T$ in the final state, namely: $W \to \tau\nu$, $Z \to e^+e^-$, WW, top pair production. The former is mainly coming from jets production. While the W-like backgrounds are modeled with Monte Carlo simulations, the QCD background is described with a data-driven technique. To extract the background fraction in each $W+ \geq n-$jet sample the $\not\!\!E_T$ distribution of candidates is fitted to background and signal templates (fig. 1-4). `Alpgen` [7] interfaced to `HERWIG` [8] has been used to generate the $W \to \tau\nu$, $Z \to e^+e^-$ backgrounds and the W signal, `PYTHIA` [9] have been used for top and WW backgrounds. The sensitivity of these template on the particular set of parton level cuts and Monte Carlo parameters has been studied. It is always below a 5% level and this effect has been included in the systematic on the background estimate. The QCD background template is extracted from the data by selecting a sample of events that pass all kinematic requirements, but which fail one or more electron identification requirements. This sample is dominated by genuine multi-jet events, but contains a few percent contamination from real EWK events. This signal component is estimated from Monte Carlo, and the resulting dependence of the background template on the assumed signal cross section is resolved iteratively to yield stable EWK, QCD and signal fractions.

Cross-checks of this method have been performed by looking to other W kinematic distributions as the W transverse mass m_T^W and the electron transverse energy E_T^e (fig. 5). In all these variables a very good agreement between data and background models has been found. Jets in $W \to e\nu$ events may occasionally originate from separate $p\bar{p}$ interactions in the same bunch crossing, promoting events to higher jet multiplicity events. The probability for this to occur is measured in minimum-bias data and the signal sample is corrected accordingly.

The total background fraction ranges from 10% at low jet multiplicity and low E_T^{jet} to 80% at high E_T^{jet} and is largely dominated by the contribution of QCD (fig. 6-7). At high jet multiplicity and high E_T^{jet}, the contribution to the background from top production is sizeable ($\geq 50\%$). In this region the uncertainty on the top pair production cross section dominates the background systematic. Elsewhere the main contribution to the uncertainty on the background fraction comes from the limited statistic of the QCD background sample.

A full detector simulation has been used to take into account selection efficiencies, coming from geometric acceptance, electron identification and $\not\!\!E_T$ and E_T^e resolution effects. The full CDF II detector simulation accurately reproduces electron acceptance and identification inefficiencies: no evidence of a difference between data and simulation have been found in the $Z \to e^+e^-$ sample. To minimize the theoretical uncertainty in the extrapolation of the measurement, the cross section has been defined for the W phase space accessible by the CDF II detector: $E_T^e > 20$GeV, $|\eta^e| < 1.1$, $\not\!\!E_T > 30$GeV and $m_T^W > 20\text{GeV/c}^2$. This eliminates the dependence on Monte Carlo models to extrapolate the visible cross section to the full W phase space. Nevertheless Monte Carlo events have been used to correct for inefficiency and boundary effects on the kinematic selection that defines the cross section. Different Monte Carlo prescriptions have been checked and the critical parameters have been largely scanned. These effects turned out to be at the 5% level at low E_T^{jet}. They have been included into the systematic uncertainty on the efficiency which is $(60 \pm 3)\%$, largely independent of the jet kitematic.

The candidate event yields, background fractions and efficiency factors are combined to form the raw W + jet cross sections. The raw cross sections are then corrected back to the hadron level jet cross sections using Monte Carlo event samples. `ALPGEN` interfaced with `PYTHIA-TUNE A` [10] provides a reasonable description of the jet and underlying event properties, and is used to determine the correction factors, defined as the ratio of the hadron level cross section to the raw reconstructed cross section.

Results are presented as both cumulative $\sigma(W \to e\nu+ \geq n-\text{jets}; E_T^{jet}(n) > E_T^{jet}(min))$ (fig. 8) and differential $d\sigma(W \to e\nu+ \geq n-\text{jets})/dE_T^{jet}$ (fig. 9) distribution where E_T^{jet} is that of the $i^{th}-$jet.

The measurement spans over three orders of magnitude in cross section and close to 200 GeV in jet E_T for the $\geq 1-$jet sample. For each jet multiplicity, the jet spectrum is reasonably well described by individually normalized `ALPGEN+PYTHIA` $W + n -$ parton samples. For $W + 2$ jet, the shapes of the cross section as a function of the 2-leading jets invariant mass (fig. 10) and angular correlation (fig. 11) are also well modeled. The systematic error is dominated by the uncertainty on the jet energy scale ($\sim 3\%$) at low E_T^{jet}, while at high energy the dominant contribution comes from the uncertainty on the background fraction, in particular from the limited statistic of the QCD background sample, as shown in fig. 12-13 for the integrated and differential cross section as a function of the leading jet E_T. We expect to reduce drastically this effect by increasing the statistic of the data sample.

In summary, we have measured the $W+ \geq n-$jet cross sections in 320 pb^{-1} of $p\bar{p}$ collisions at $\sqrt{s} = 1.96$ TeV, including events with up to 4 or more jets produced in association with the W boson. The cross sections, defined in a limited W decay phase space, have otherwise been fully corrected for all known detector effects. Preliminary comparisons show reasonable agreement between the measured cross sections and the predictions of matched Monte Carlo samples.

References

[1] M.A. Dobbs *et al.*, hep-ph/0403045, and reference therein.

[2] D. Acosta *et al.* [CDF Collaboration], Phys. Rev. **D 63** (2001) 072003.

[3] D. Acosta *et al.* [CDF Collaboration], Phys. Rev. Lett. **81** (1998) 1367.

[4] D. Acosta *et al.* [CDF Collaboration], Phys. Rev. **D 71** (2005) 032001.

[5] F. Abe *et al.* [CDF Collaboration], Phys. Rev. **D 45** (1992) 1448.

[6] A. Bhatti *et al.*, hep-ex/0510047.

[7] M. Mangano *et al* JHEP **0207** 012 (2002).

[8] G. Corcella *et al.*, JHEP **0101** (2001) 010, HERWIG 6.4.

[9] T. Sjostrand *et al.*, Comput. Phys. Commun. **135** (2001) 238, PHYTIA 6.203.

[10] T. Affolder *et al.* [CDF Collaboration], Phys. Rev. **D 65** (2002) 092002.

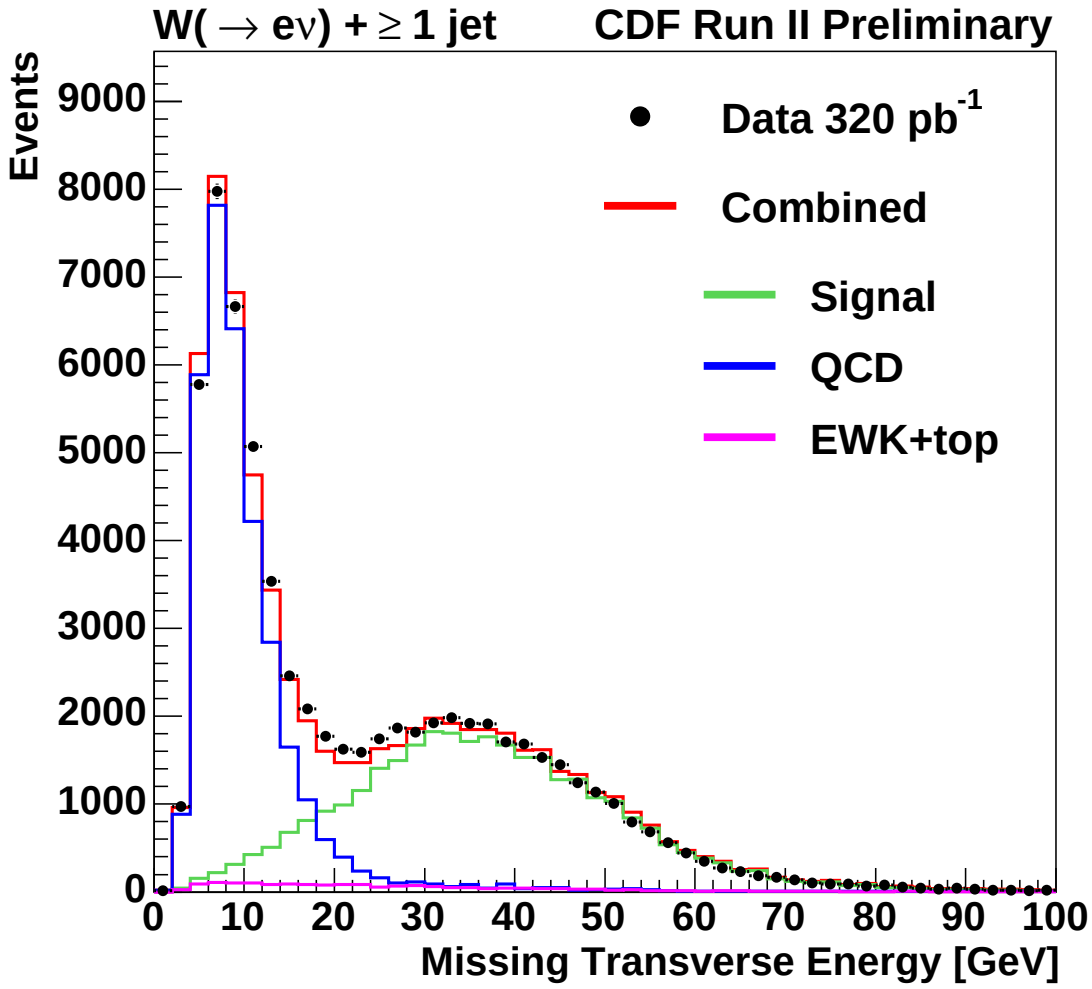

Figure 1: Missing transverse energy in the $W+ \geq 1$ jet sample. The missing transverse energy distribution in data is fitted to background and signal templates to extract the background normalization. The blue histogram is the template for the qcd background, extracted from data. The green histogram is the signal template and the purple one is the template for all the other backgrounds: $W \rightarrow \tau\nu$, $Z \rightarrow ee$, WW, *top*. The red histogram is the combined template that best fits the data.

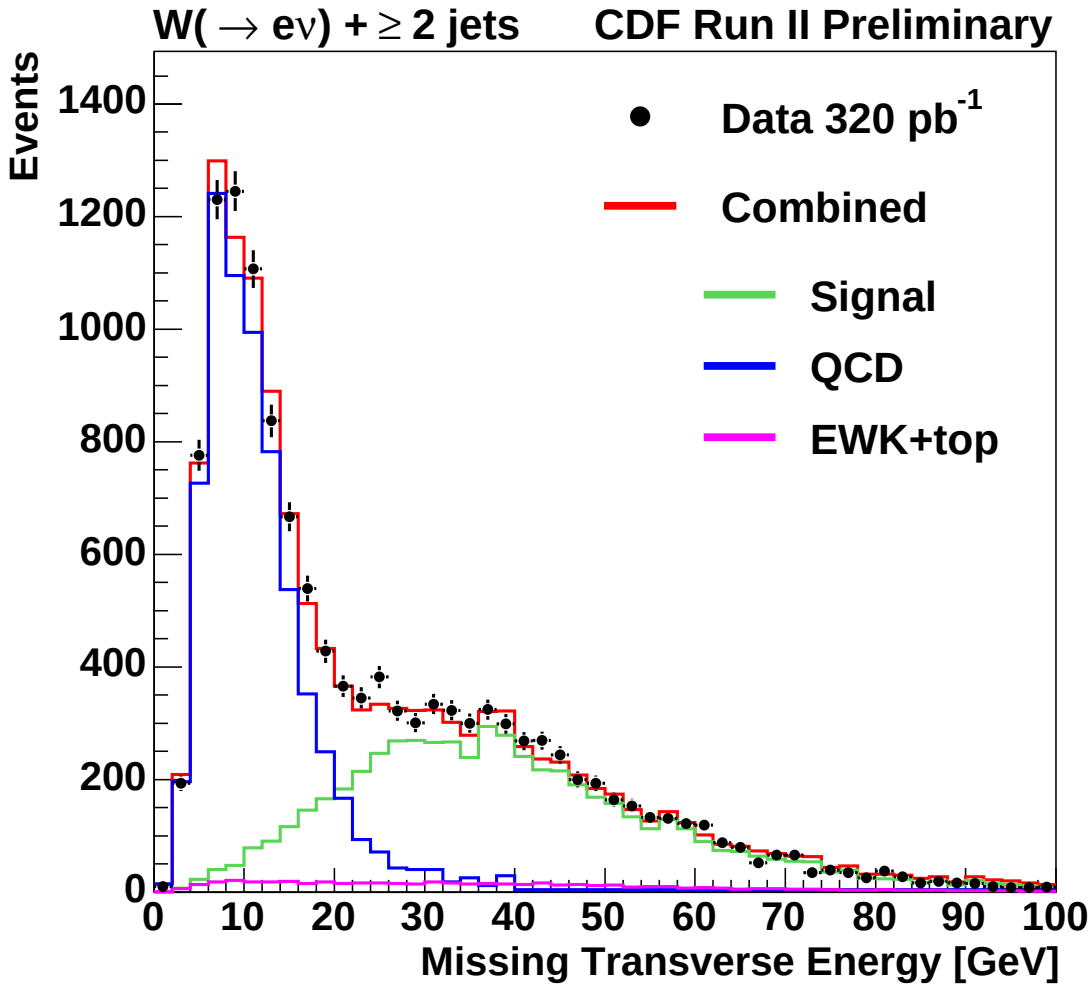

Figure 2: Missing transverse energy in the $W+ \geq 2$ jet sample. The missing transverse energy distribution in data is fitted to background and signal templates to extract the background normalization. The blue histogram is the template for the qcd background, extracted from data. The green histogram is the signal template and the purple one is the template for all the other backgrounds: $W \rightarrow \tau\nu$, $Z \rightarrow ee$, WW, *top*. The red histogram is the combined template that best fits the data.

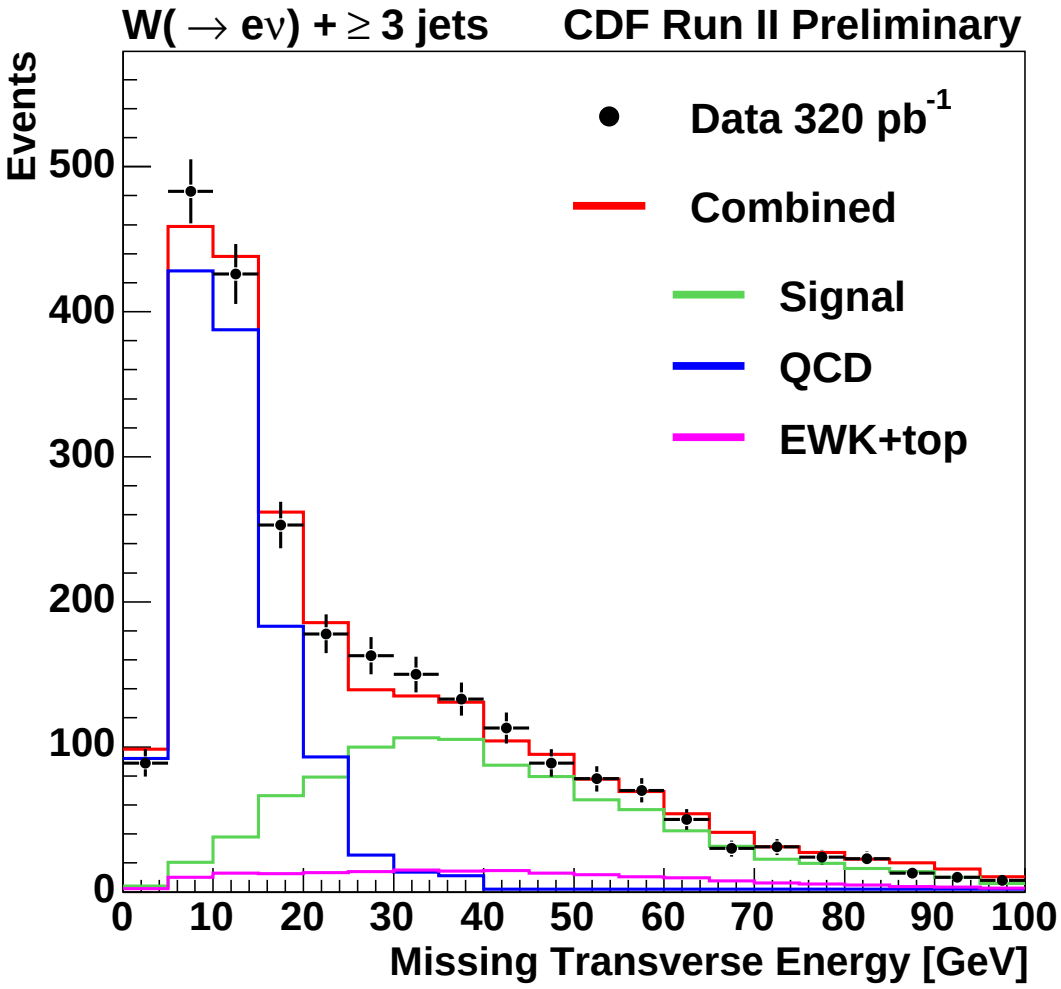

Figure 3: Missing transverse energy in the $W+ \geq 3$ jet sample. The missing transverse energy distribution in data is fitted to background and signal templates to extract the background normalization. The blue histogram is the template for the qcd background, extracted from data. The green histogram is the signal template and the purple one is the template for all the other backgrounds: $W \rightarrow \tau\nu$, $Z \rightarrow ee$, WW, *top*. The red histogram is the combined template that best fits the data.

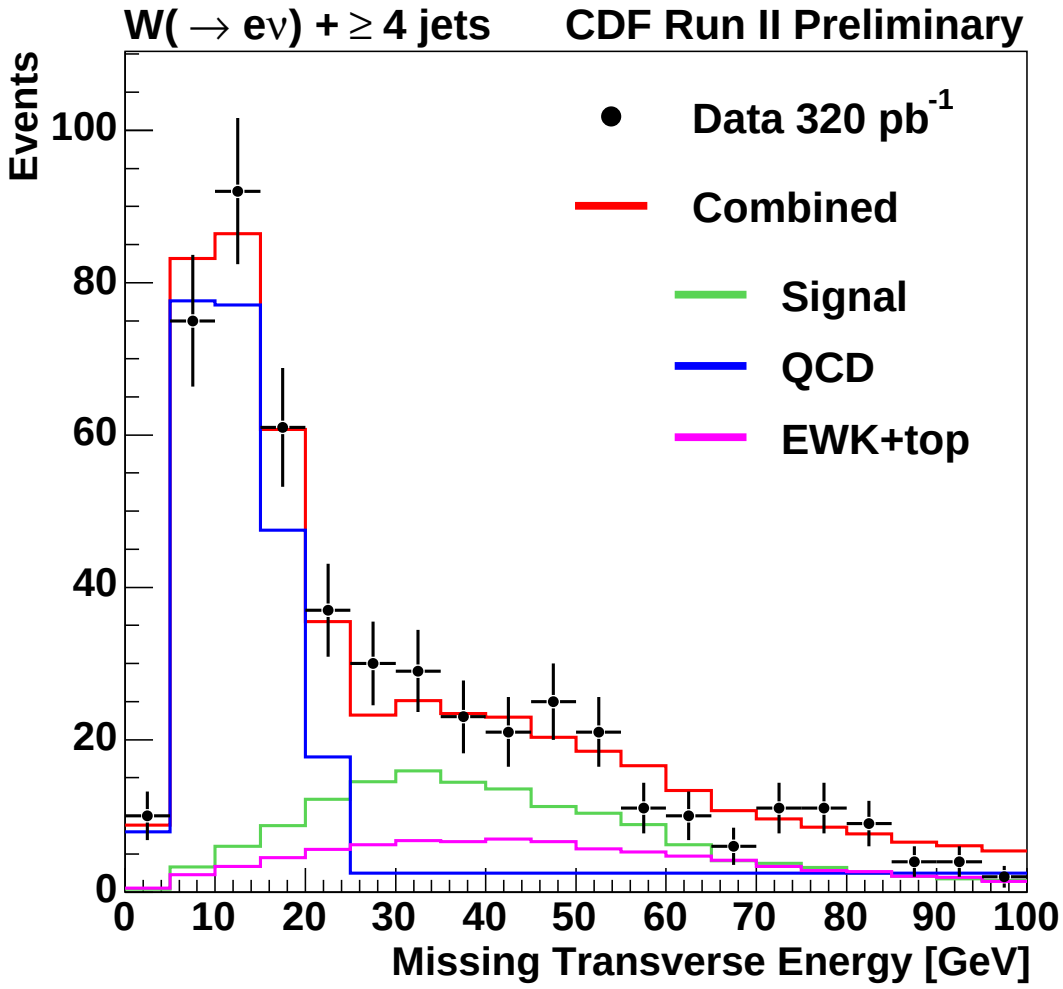

Figure 4: Missing transverse energy in the $W+ \geq 4$ jet sample. The missing transverse energy distribution in data is fitted to background and signal templates to extract the background normalization. The blue histogram is the template for the qcd background, extracted from data. The green histogram is the signal template and the purple one is the template for all the other backgrounds: $W \rightarrow \tau\nu$, $Z \rightarrow ee$, WW, *top*. The red histogram is the combined template that best fits the data.

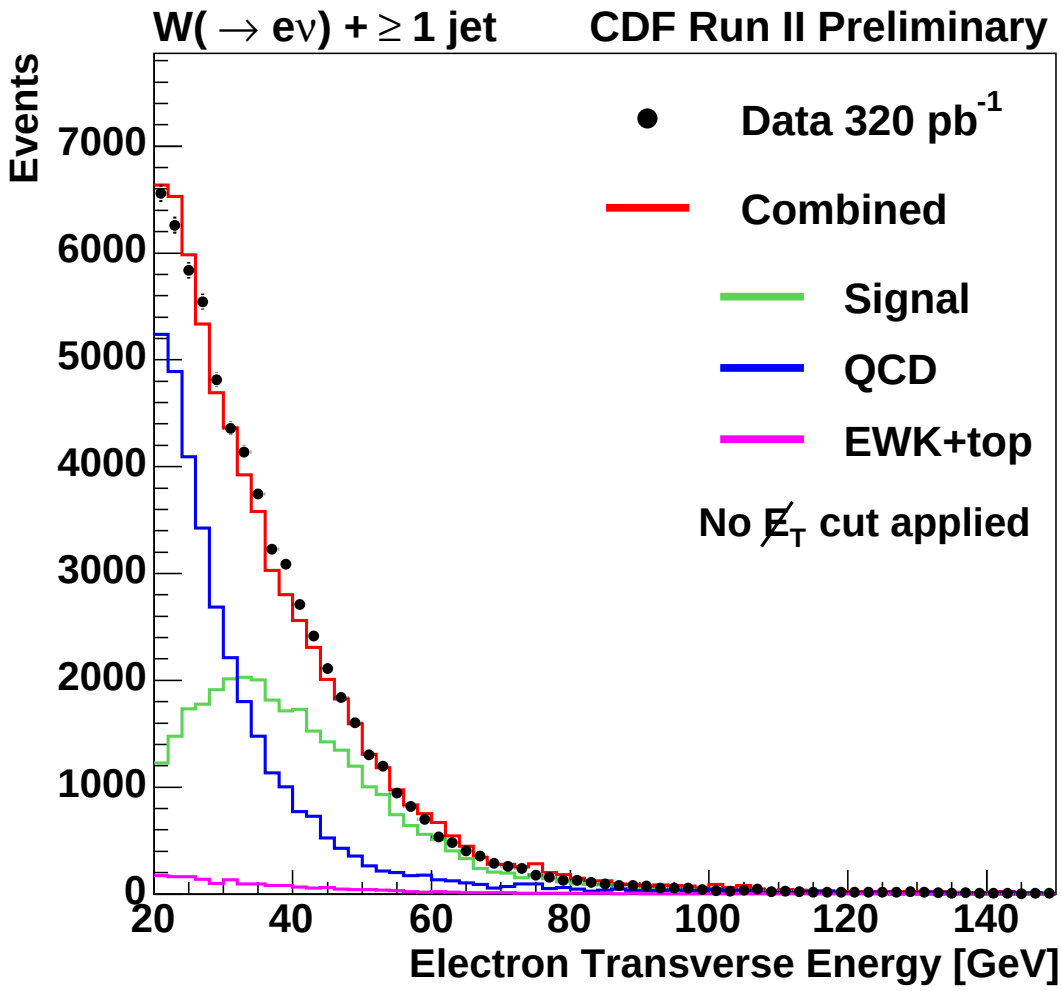

Figure 5: Electron transverse energy in the $W+ \geq 1$ jet sample. The electron transverse energy distribution in data is compared to the signal and background templates normalized to the fractions extracted from the missing transverse energy fit.

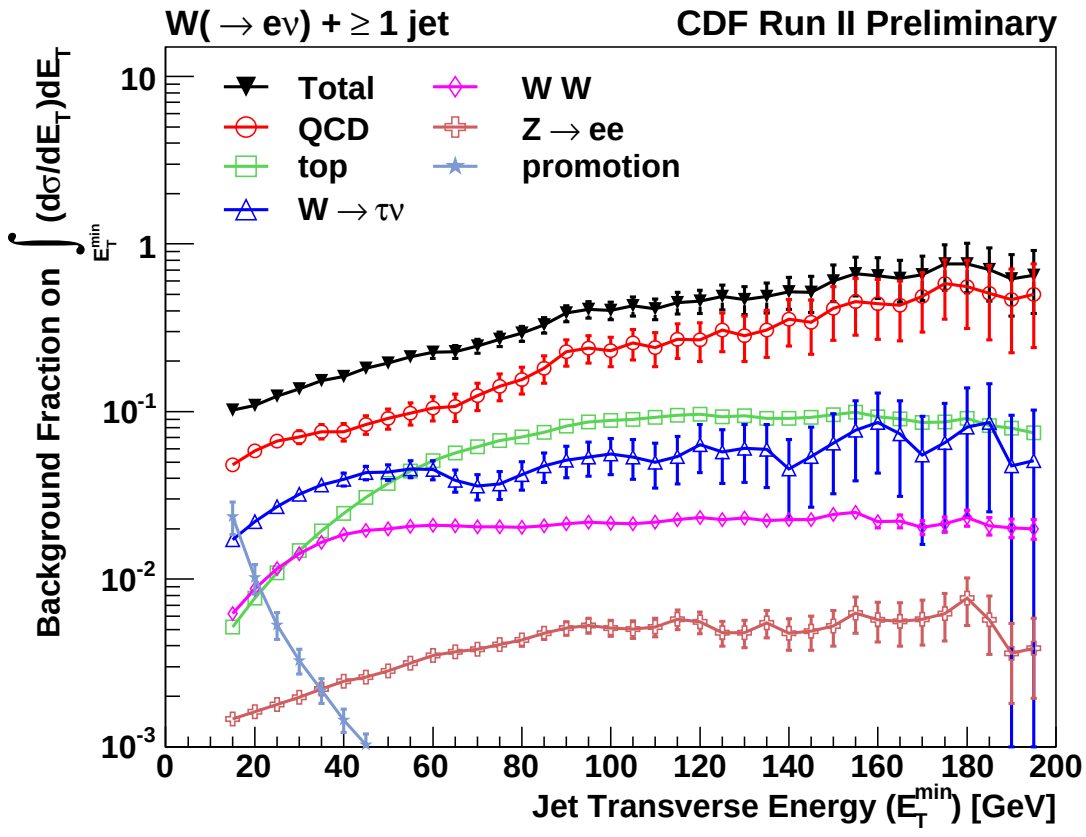

Figure 6: Background fraction as a function of the leading jet minimum transverse energy in the $W+ \geq 1$ jet sample.

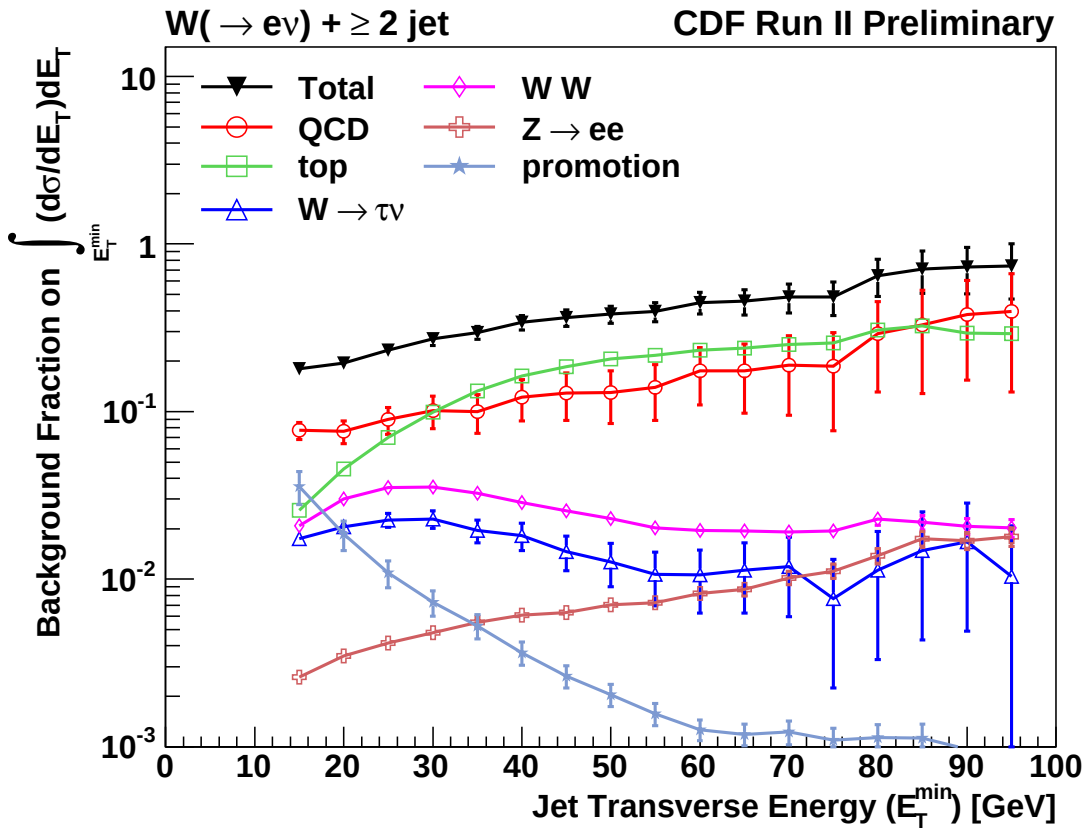

Figure 7: Background fraction as a function of the leading jet minimum transverse energy in the $W+ \geq 2$ jet sample.

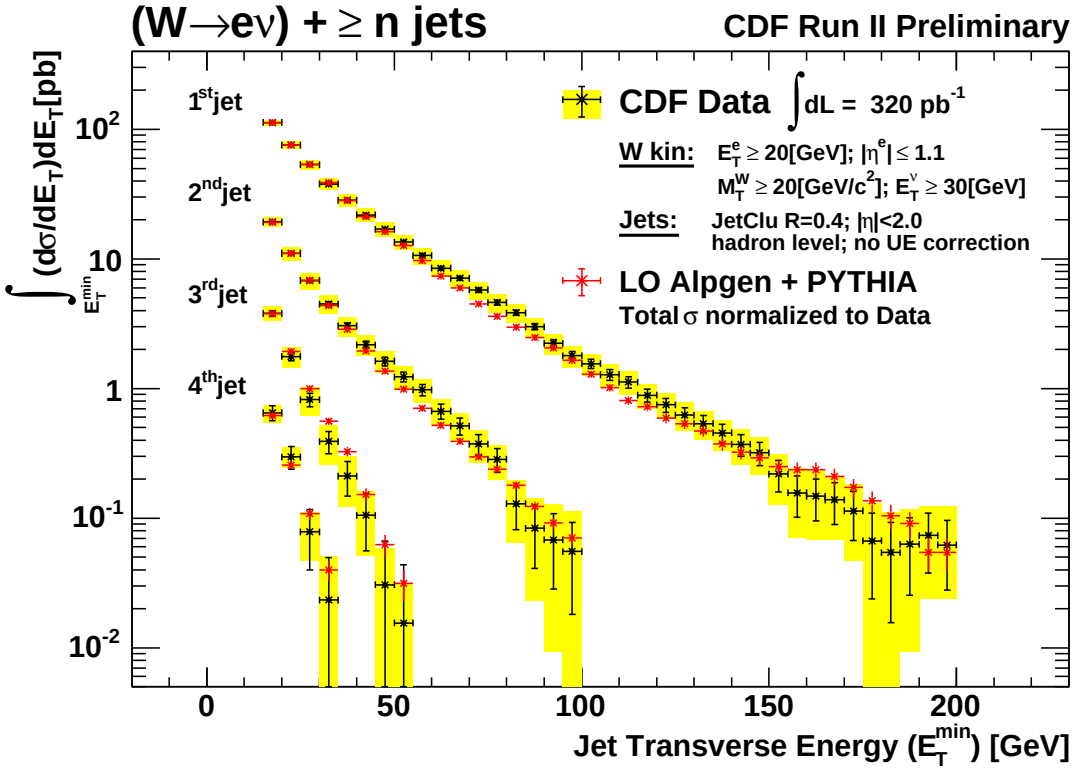

Figure 8: Cumulative cross section $\sigma(W \rightarrow e\nu + \geq n - \text{jets}; E_T^{jet}(n) > E_T^{jet}(min))$ as a function of the minimum $E_T^{jet}(min)$ for the first, second, third and fourth inclusive jet sample. Data are compared to `Alpgen`+`PYTHIA` predictions normalized to the measured inclusive cross section in each jet multiplicity sample.

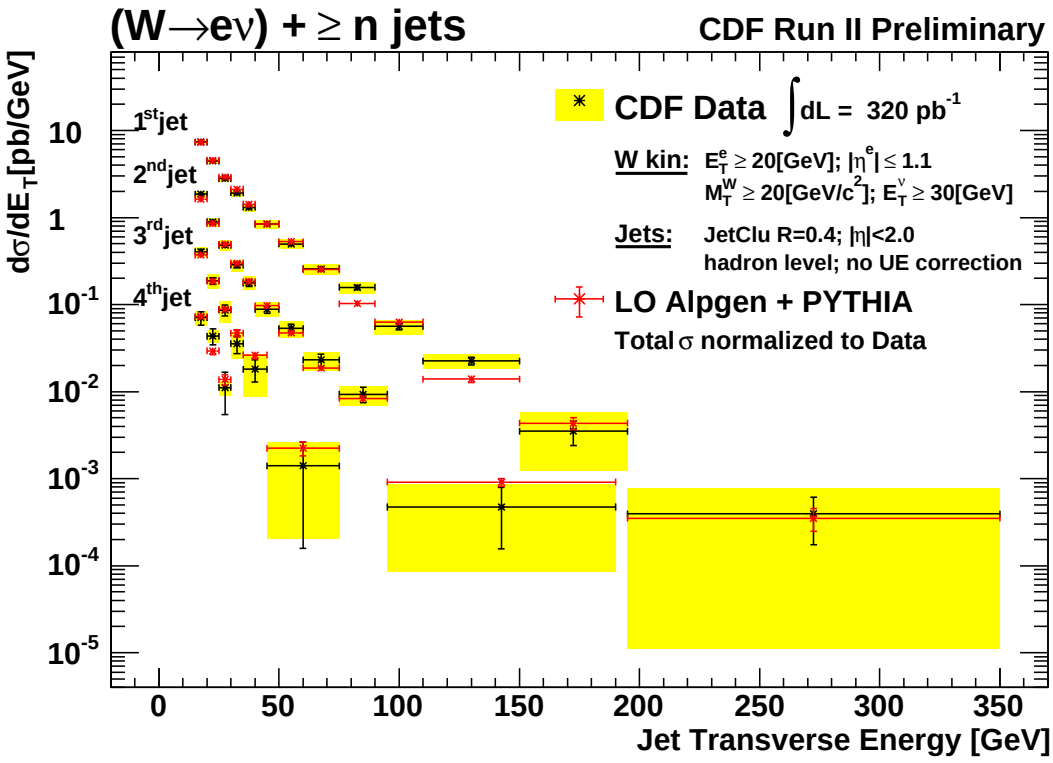

Figure 9: Differential cross section $d\sigma(W \rightarrow e\nu + \geq n - \text{jets})/dE_T^{jet}$ (Right) for the first, second, third and fourth inclusive jet sample. Data are compared to `Alpgen`+`PYTHIA` predictions normalized to the measured inclusive cross section in each jet multiplicity sample.

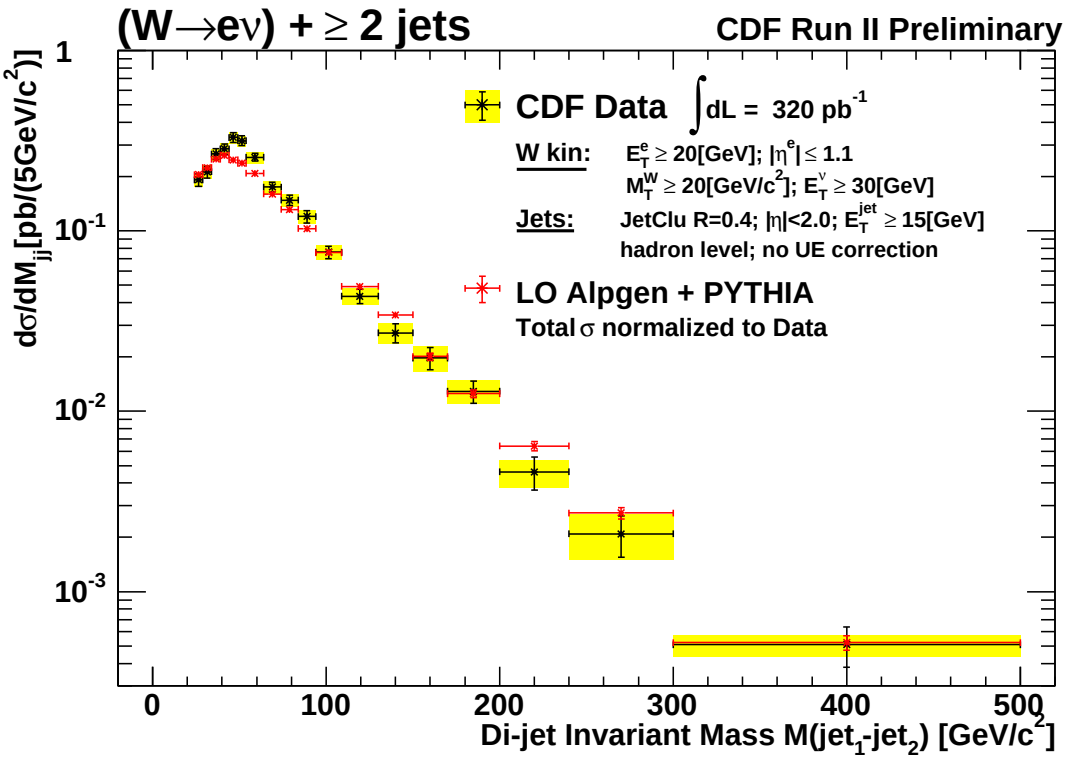

Figure 10: Differential cross section $d\sigma(W \rightarrow e\nu + \geq 2 - \text{jets})/dM_{j1j2}$ as a function of the invariant mass of the 2 leading jets in the $W+ \geq 2$ jet event. Data are compared to `Alpgen`+`PYTHIA` predictions normalized to the measured inclusive cross section.

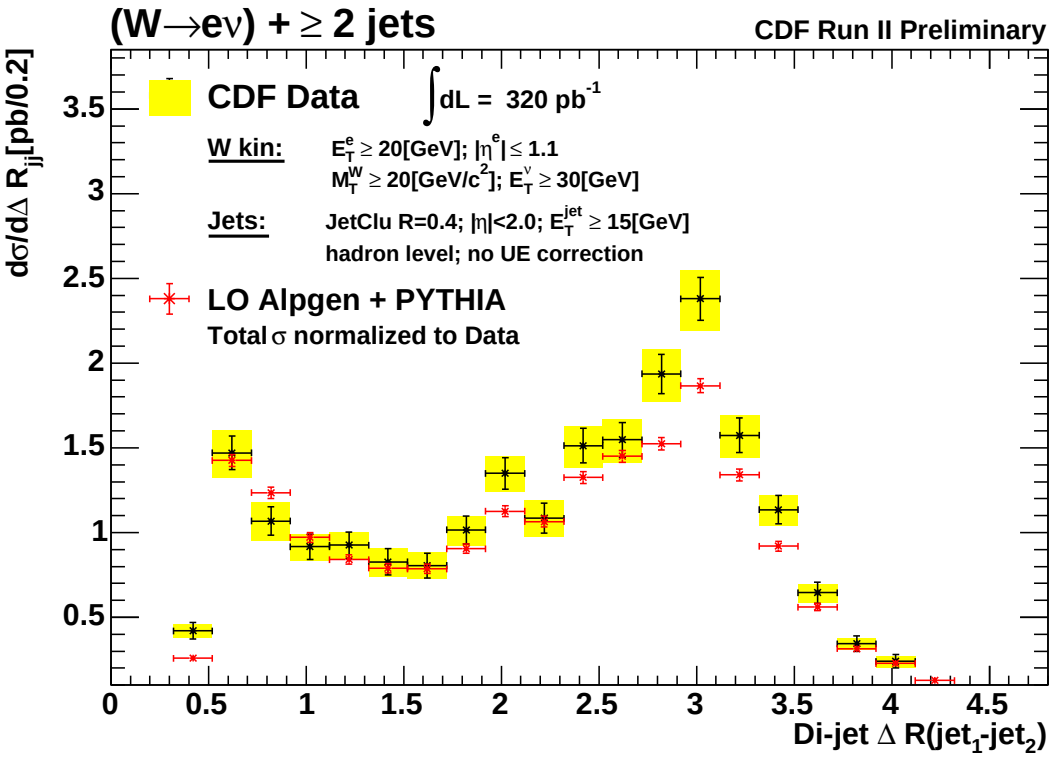

Figure 11: Differential cross section $d\sigma(W \rightarrow e\nu + \geq 2 - \text{jets})/dR_{j1j2}$ as a function of the invariant mass and angular separation of the 2 leading jets in the $W+ \geq 2$ jet event. Data are compared to `Alpgen`+`PYTHIA` predictions normalized to the measured inclusive cross section.

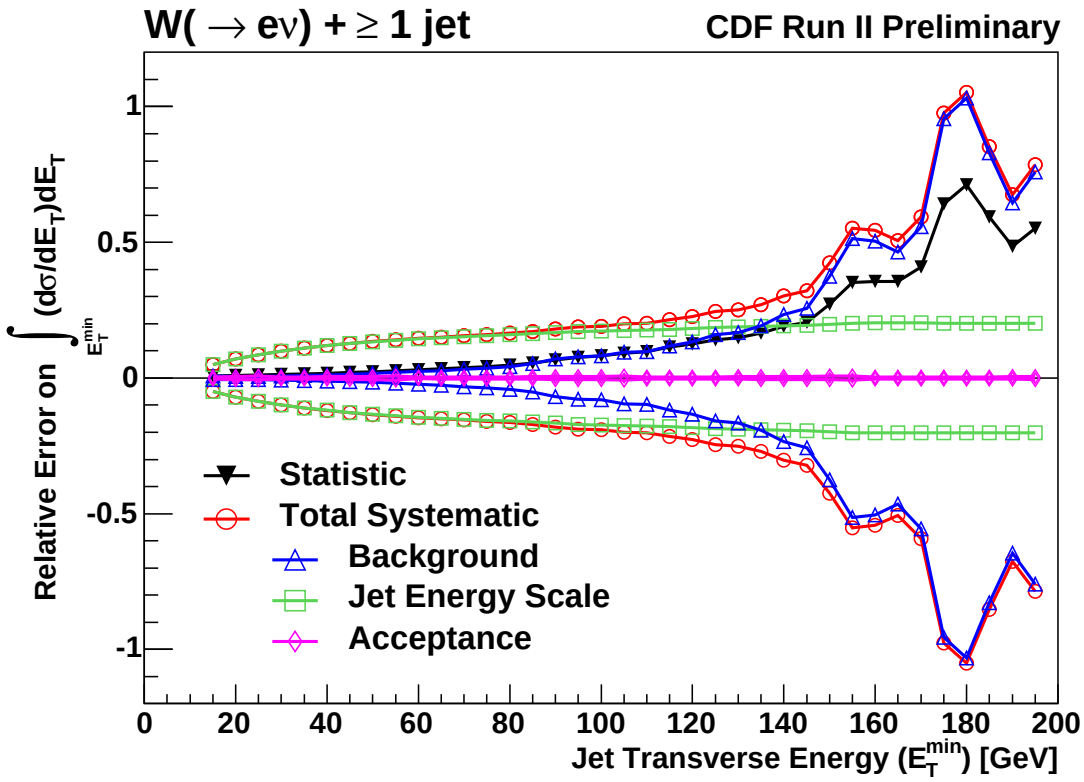

Figure 12: Error breakdown for the cumulative cross section as a function of the leading jet minimum transverse energy in the $W+ \geq 1$ jet sample.

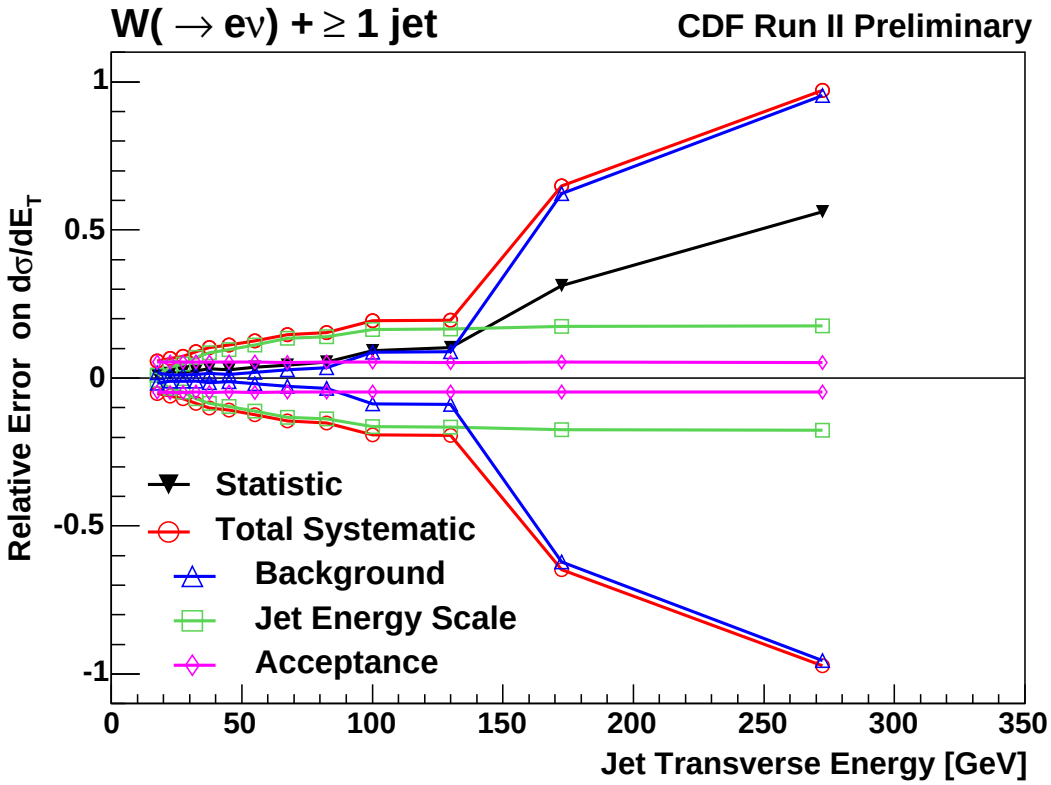

Figure 13: Error breakdown for the differential cross section as a function of the leading jet transverse energy in the $W+ \geq 1$ jet sample.